

# IDENTIFICATION, MODELING AND CONTROL OF TEMPERATURE FIELDS IN CONCRETE STRUCTURES

Grzegorz Knor\* and Jan Holnicki-Szulc\*

\*Institute of Fundamental Technological Research, Polish Academy of Sciences  
ul. Pawińskiego 5B; 02-106 Warsaw, Poland  
e-mail: <gknor@ippt.pan.pl> webpage: <http://www.ippt.pan.pl>

**Keywords:** inverse heat transfer problem, fly ash, pipe cooling system

**Abstract.** *Cement production is an energy-intensive process that releases large amounts of carbon dioxide into the atmosphere. Thus the reduction of cement content in concrete structures is equivalent to the decrease of CO<sub>2</sub> emission. Therefore, during recent years there has been an increasing stress on utilization of various by-products as substitutes for cement in the concrete materials. The world's largest lignite-fired power station is in Poland. It is situated near Bełchatów and produces huge amounts of high calcium fly ashes which can be added to concrete. However, the main problem is variation with time of the chemical composition of fly ashes which makes it necessary to test each individual supply of ash. In our research the impact of high calcium fly ash on the hydration process (i.e. reaction kinetics and heat production) is tested. Moreover, we have developed a new method for determination of concrete thermal properties, based on the point temperature measurement, as well as the solution of the inverse heat transfer problem. Temperature measurements during concrete hydration are performed using patented device for a three-day concrete hardening heat measurement. So it is possible to examine each concrete mixture (i.e. to determine its thermal properties) and next calculate the temperature and stress fields in hardening massive structure made of this mixture. For modelling thermo-mechanical phenomena the in-house FEM software has been developed. Moreover, this software provides the opportunity to design an optimal pipe cooling system to minimize the risk of cracking.*

## 1 INTRODUCTION

Polish Research Program<sup>1</sup> for the coming years is closely related to security, stability, usability and reliability of buildings. This requires the development of new structures and materials safe both for health and the environment and revealing high time durability. Therefore it is necessary to develop a new generation of construction materials showing high strength and thermal properties and use new technologies making it possible to design and modify the structure of the materials in order to obtain the desired properties. Moreover, the high exploitation of natural resources and high emissions of carbon dioxide from cement production all over the world (in 2011 the world production of hydraulic cement was 3,400 million tonnes, see Fig. 1) forced the producers to seek new solutions. One of the ideas to reduce environmental and economical costs is to use the by-products of different kind, which could replace some of cement in the masonry mortar. A wide range of supplementary cementitious materials can be taken into

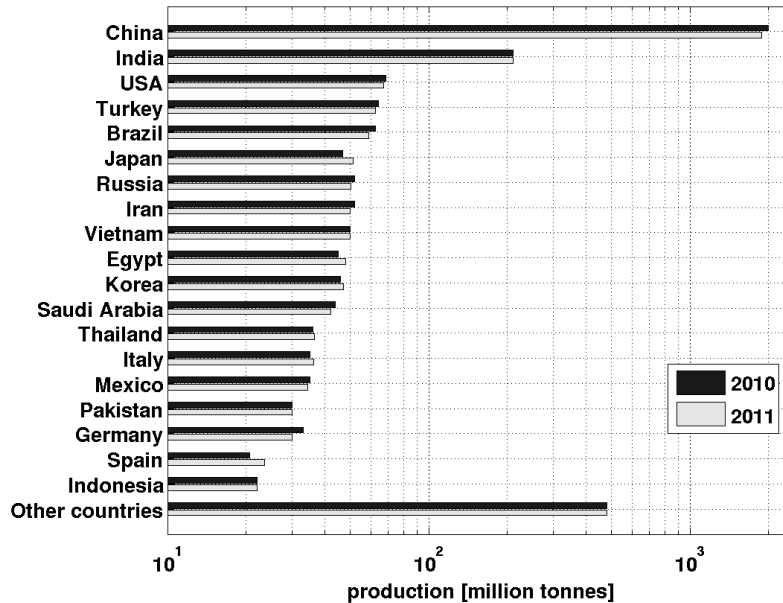


Figure 1: Global cement production in 2010 & 2011<sup>2</sup>.

account, including ground granulated blast furnace slag, metakaolin, recycled plastic, scrap tires, demolition of buildings, usually makes it possible to limit the extraction of primary raw materials. Obviously cement with some additions reveals properties different from pure cement. The comparison of chemical and physical properties of Portland cement with those containing most popular cement substitutes is shown in Table 1. Comprehensive description of listed additions can be found in Siddique's books<sup>4,5</sup>. Unfortunately, the properties of some materials are only qualitatively but not quantitatively determined, because of labile composition, which can vary in time and depend on chemical composition of additions origin. Addition of calcareous fly ash<sup>6</sup> is the case. In Bełchatów (Poland) the world's second largest fossil power plant (and the world's largest lignite-fired power station) is located which generates huge amounts of fly ashes, especially calcareous fly ashes. In this paper we would like to present the complete procedure which consists of three parts: identification, modelling and temperature control in concrete structure made with high-calcium fly ashes. These parts are combined into in-house, based on FEM formulation software TMC.

In this case identification is referred to as the determination of concrete thermal parameters by means of the inverse heat transfer problem (IHTP) solution. As mentioned above the properties of concrete with calcareous fly ash vary in time<sup>7</sup> and it is necessary to determine the thermophysical properties of such concrete mixtures due to accurate modeling. The heat of hardening, thermal conductivity and specific heat are determined on the basis of point temperature measurements in a cylindrical mold<sup>8</sup> followed by solution of optimization problem using direct search algorithm<sup>9</sup>.

The second part is a numerical model of temperature field in hardening concrete. In the aforementioned inverse problem the one dimensional direct heat conduction problem for early age concrete must be defined. In the case of more complex shapes than a cylindrical mould, from which measurements are used for IHTP solution, the heat transfer model has been developed. As a result thermal stress field can be calculated, based on the prior calculated temperature field, however, in this paper the thermomechanical aspect has not been considered.

The first part – control – deals with the cooling system in concrete structure. Cooling system embraces both precooling and postcooling of concrete. For example, it is possible to estimate the placing temperature of concrete, such that potential tensile strain does not exceed the strain capacity of the concrete, on the basis of the following equation<sup>10</sup>:

$$T_{ci} = T_{cf} + \frac{100C}{e_t \cdot K_r} - \Delta T_c \quad (1)$$

(all symbols are described in Table 2).

It means that by precooling it is possible to reduce thermal stresses in massive concrete structure. Precooling can be achieved, for example, by shading the aggregate stockpile, incorporating

crushed ice into water mixed in or the use of liquid nitrogen. The first attempts to introduce such solution were made during the construction on Norfolk Dam in 1941-45<sup>11</sup>. This approach, however, has not been considered in this article. In this paper an embedded pipe cooling system is discussed. Historically such solution of postcooling was used for the first time over 80 years ago during Hoover Dam construction<sup>11</sup> and it has been still used. The simplified model of pipe network in massive concrete structure has been developed. The proposed model is an extension of other authors works<sup>12,13,14</sup>. It is used to design the optimal pipe cooling system.

The complete list of symbols used in this paper is shown in Table 2.

Property	Portland cement	Class F fly ash	Class C fly ash	Slag cement	Silica Fume
SiO <sub>2</sub> content, %	21	52	35	35	85 to 97
Al <sub>2</sub> O <sub>3</sub> content, %	5	23	18	12	0
Fe <sub>2</sub> O <sub>3</sub> content, %	3	11	6	1	0
CaO content, %	62	5	21	40	<1
Fineness as surface area, [m <sup>2</sup> /kg]	370	420	420	400	15,000 to 30,000
Specific gravity	3.15	2.38	2.65	2.94	2.22
General use in concrete	Primary binder	Cement replacement	Cement replacement	Cement replacement	Property enhancer

Table 1: Comparison of chemical and physical properties of Portland cement and most popular cement replacements<sup>3</sup>.

Symbol	Description
$T_c$	concrete temperature
$T_{ci}$	placing temperature of concrete
$T_{cf}$	final stable temperature of concrete
$T_{c0}$	initial temperature of concrete
$\Delta T_c$	initial temperature rise of concrete
$T_w$	water temperature
$T_{w0}$	initial temperature of water
$T^e$	measured temperature
$T^n$	calculated temperature
$\rho_c$	concrete density
$\rho_w$	water density
$k_c$	concrete conductivity
$k_w$	water conductivity
$c_c$	specific heat of concrete
$c_w$	specific heat of water
$S$	rate of heat production per unit volume
$Q$	water flow rate
$C$	strain capacity (in millionths)
$e_t$	coefficient of thermal expansion per deg of temperature (in millionths)
$K_r$	degree of restraint (in per cent)
$\alpha$	vector of sought parameters in IHTP
$M$	number of sensors

Symbol	Description
$l$	number of measurements
$\gamma$	regularization parameter
$t$	time
$t_e$	equivalent time
$R_g$	gas constant
$E_a$	activation energy
$H$	heat transfer coefficient between the pipe and concrete
$r$	radius
$x,y,z$	spatial coordinates
$a$	pipe radius
$R$	radius of a concrete element

Table 2: Notation.

## 2 MATERIALS & MEASUREMENTS

The experiment has been carried out for series of concrete mixtures, in which 0%, 15%, 30%, 60% or 100% of pure cement was replaced by high calcium fly ash. The mixtures also differ in the type and content of coarse aggregates (crushed granodiorite, limestone chippings and amphibolite aggregate) were used. The water/binder ratio was set to 0.5-0.6. The details of composition of each mixture can be found in the project scientific report<sup>15</sup>.

The measurements were performed in three configurations: 1D, 2D and 3D. Figure 2 shows schema of cylindrical (1D) and trapezoidal (2D) mould. Thermal isolation of the moulds was made of polyethylene foam and polystyrene foam, in order to minimize the heat loss through the walls (except for the upper surface, through which a free exchange of heat occurs). Figure 3 shows schema of cuboid (3D) mould with an approximate volume 0.5 m<sup>3</sup>. This mould allows the configuration of insulation on the walls to be changed, so it is possible to examine the same concrete mixture in different conditions. The semiconductor temperature sensors are used to measure the temperature (4, 7 and 8 sensors for 1D, 2D and 3D case, respectively). The data acquisition system consists of data logger and set of sensors and it records temperature data automatically with high time resolution. In each case the ambient temperature is also recorded.

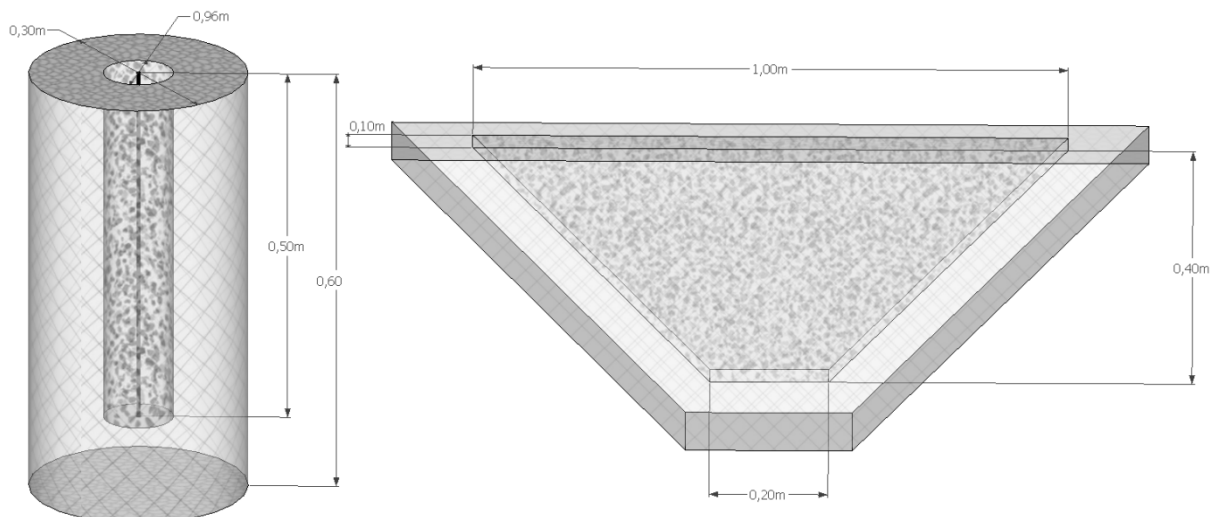


Figure 2: Schema of cylindrical and trapezoidal mould for temperature measurements.

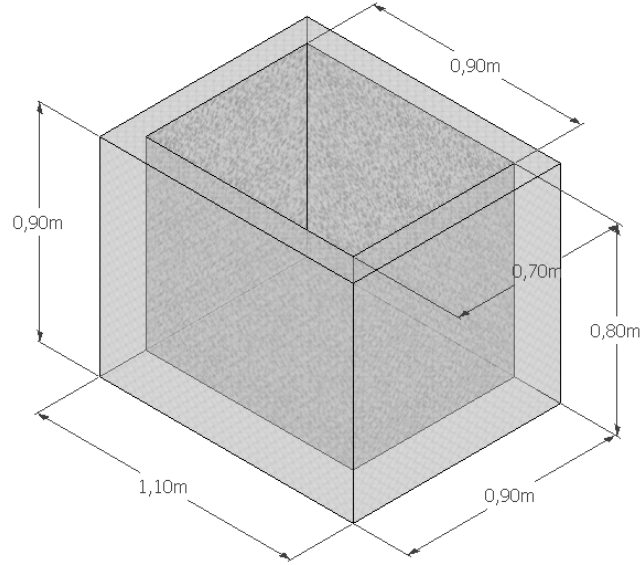


Figure 3: Schema of cuboid mould for temperature measurements during self-heating of concrete.

### 3 IDENTIFICATION

#### 3.1 Mathematical formulation

Solution of heat conduction equation in case of early age concrete is technically difficult and time-consuming task. In this approach  $k_c$ ,  $c_c$  and  $S$  are parameterized as piecewise linear function of set of unknown parameters  $\alpha$  and equivalent time  $t_e$ :

$$\begin{aligned} S &= S(\alpha, t_e) \\ c_c &= c_c(\alpha, t_e) \\ k_c &= k_c(\alpha, t_e) \end{aligned} \quad (2)$$

where equivalent age of concrete is defined as:

$$t_e(t) = \int_0^t \exp\left(\frac{E_a}{R_g} \left(\frac{1}{293} - \frac{1}{T_c + 273}\right)\right) dt' \quad (3)$$

and the  $E_a/R_g$  ratio is defined as:

$$\frac{E_a}{R_g} = \begin{cases} 4000 \left[\frac{1}{K}\right] & \text{if } T_c > 20^\circ\text{C} \\ 4000 + 175(20 - T) \left[\frac{1}{K}\right] & \text{if } T_c \leq 20^\circ\text{C} \end{cases} \quad (4)$$

The numerical values of  $\alpha$  parameters are determined by means of the inverse problem solution based on temperature measurements in cylindrical mold<sup>8</sup>.

$$E(\alpha) = \sum_{m=1}^M \sum_{i=1}^I (T_{im}^e - T_{im}^n)^2 + \gamma \sum_{p=1}^P \alpha_p^2 \quad (5)$$

where the Tikhonov regularization is applied (second term in Eq. 5) to stabilize the solution of inverse problem.

### 3.2 Numerical implementation

In order to find the minimum of the objective function defined by Eq. 5 MATLAB routine *pattern search* was used. Routine *pdepe* was utilized to calculate temperature distribution in cylindrical mould. In temperature model Dirichlet boundary conditions and information about the heat loss through wall<sup>8</sup> was introduced. Optimization problem for each concrete mixture was solved at least twenty times with random initial mesh size<sup>9</sup> and the results to be presented further on are the averages of these solutions. The order of selecting the directions at which algorithm converges to the minimum value, was also randomly chosen. Initial values of  $\alpha$  parameters for the heat source function were selected as the constants for each individual concrete compositions. In addition, it was assumed that for the time periods exceeding 72 hours the heat value decreases linearly to zero. The initial values of specific heat and thermal conductivity coefficients were random according to the following scheme:

- Coefficient of thermal conductivity:  $k_0 = rand() + 1.5$
- Heat capacity:  $c_{p0} = 100 \cdot rand() + 1000$

where *rand()* means a pseudorandom number in the range of [0-1].

Number of iterations (and the function calls) differed significantly for each execution of the algorithm. Figure 4 shows the relationship between the number of iterations and function calls. The minimum number of iterations was 73 and the maximum – 1937, the corresponding values of function calls were 2292 and 70663, respectively. All calculations, due to their complexity, were performed on a Linux cluster at IPPT PAN.

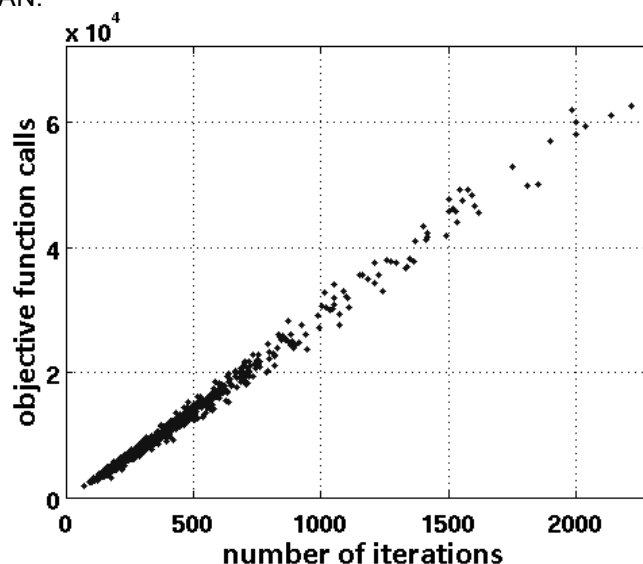


Figure 4: Optimization.

## 4 MODELING

### 4.1 Mathematical formulation

In order to solve the inverse problem, first the direct problem must be formulated. In our approach a standard heat conduction equation is used (the influence of both the humidity and object deformation is neglected):

$$\rho_c c_c \frac{\partial T}{\partial t} = k_c \Delta T_c + S \quad (6)$$

Determination of the temperature field using Eq. 6 requires defining the boundary condition and temperature distribution in the concrete structure at time  $t = 0$ . It is important to bear in mind that all values of thermal properties used in Eq. 6 are changing during hydration process. It means that adapted model of temperature evolution in concrete is non-linear, because according to Eq. 3, the rate of hydration process depends on temperature (and as a result also on the position).

## 4.2 Numerical implementation

The numerical implementation of temperature model can be split into two independent parts: one- and two-dimensional approach (for 3D case – Fig. 3 – two-dimensional model is used<sup>16</sup>). To solve one-dimensional problem (for the purposes of IHTP) the method of lines, implemented as a *pdepe* MATLAB routine, is used and to solve two-dimensional issue FEM model is implemented as in-house software TMC. In order to take into account the effect of the equivalent age of concrete it is more convenient to write integral (3) as an ordinary differential equation:

$$\frac{dt_e}{dt} = \exp\left(\frac{E_a}{R_g} \left(\frac{1}{293} - \frac{1}{T_c + 273}\right)\right) \quad (7)$$

and solve it simultaneously with Eq. 6.

## 5 CONTROL

### 5.1 Mathematical formulation

The heat conduction equation for concrete (6) can be conjugated with heat equation for water in cooling pipes in order to calculate the influence of pipe network on temperature distribution in massive concrete structure. The simplified model of concrete construction, which consists of series of equispaced pipes, is adopted<sup>13</sup>. Stream of water in each pipe is directed opposite to that in the adjacent pipe. Figure 5 (drawn out of scale) shows the configuration of the system. Single concrete sleeve of length  $L$  and radius  $R$  with centrally located pipe of radius  $a$  is considered. The length of concrete sleeve is significantly greater than its radius. The assumption has been made that temperature gradient is 0 at the midpoint between the pipes. This simplification permits the adoption of insulated boundary conditions. Moreover, it is more convenient to write heat conduction equations for both media in cylindrical coordinates. The next important assumption is a turbulent water flow, so that the temperature of water in the pipe does not depend on its radial position. The heat exchange at the boundary between concrete and piped water can be described by the following equation:

$$k_w \frac{\partial T_w}{\partial r} \Big|_{r=a} = H(T_c|_{r=a} - T_w) \quad (8)$$

where heat transfer coefficient  $H$  involves pipe thickness and thermal conductivity<sup>14</sup>.

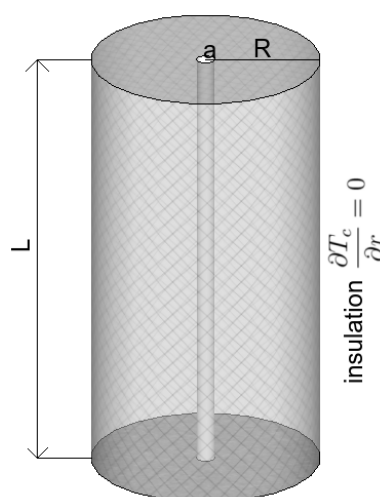


Figure 5: Cooling pipe in long cylindrical slab of concrete (drawn out of scale).

Bearing in mind these assumptions and neglecting the less important terms, the heat equations for pipe cooling system in concrete structure can be written<sup>12,13</sup>:

$$\rho_c c_c \frac{\partial T_c}{\partial t} = k_c \frac{1}{r} \frac{\partial}{\partial r} \left( r \frac{\partial T_c}{\partial r} \right) + S \quad (9)$$

$$\frac{\partial T_w}{\partial z} = \frac{2\pi H a}{Q \rho_w c_w} (T_c|_{r=a} - T_w)$$

Of course set of equations (9) is conjugated with Eq. (6) in order to take into account the effect of temperature on thermophysical properties of concrete.

The boundary conditions are expressed as heat exchange for  $r = a$ :

$$k_c \frac{\partial T_c}{\partial r} = H(T_c - T_w) \quad (10)$$

insulation for  $r = R$ :

$$\frac{\partial T_c}{\partial r} = 0 \quad (11)$$

and in the case of water, the inlet temperature is specified:

$$T_w(t, z = 0) = T_{w0} \quad (12)$$

To complete the description of the problem the initial conditions have to be specified:

$$\begin{aligned} T_c(t = 0, r) &= T_{c0} \\ T_w(t = 0, z) &= T_{w0} \\ t_e(t = 0) &= 0 \end{aligned} \quad (13)$$

This formulation allows the temperature distribution for specified configuration to be calculated, but the main goal is to design an optimal cooling system in concrete structure. Therefore, based on this formulation an optimization problem is defined and solved. In this paper we solve simultaneously the problem of optimal pipe size, pipe placing and inlet water temperature with respect to minimizing the temperature gradient.

## 5.2 Numerical implementation

Numerical implementation of this task is similar to the solution proposed in previously cited article<sup>12</sup>. MATLAB routine *pdepe* was used to solve one-dimensional heat equation in concrete (Eq. 9) in cylindrical coordinate system. The main difference is that heat equation is coupled with equivalent age equation (Eq. 7) and moreover the heat source  $S$  comes from IHTP solution. Smoothing spline<sup>17</sup> method was used to interpolate heat source data obtained from 1D measurements and IHTP solution. Additionally, this approach was combined with optimization routines to find an optimal cooling system. The goal of optimization is to find such conditions under which average temperature difference per unit length in modelled structure will be the lowest possible. The temperature difference per unit length [°C/m] is defined at each point of concrete as a temperature difference between the point with the lowest temperature divided by a distance from it. It is obvious that unconstrained optimization results would be: the pipe radius as large as possible, with as small as possible amount of concrete and inlet water temperature close to 0°C. So it is necessary to add to the objective function some technical constrains. This issue is discussed in the result section.

## 6 EXPERIMENTAL RESULTS

The example results of temperature measurements in concrete in cylindrical, trapezoidal and cuboid mould are shown in Figs. 6, 7 and 8. The positions of temperature sensors are described in the legend in each figure. The composition of concrete mixtures, for which results are



presented, are shown in Table 3. In mixture A multicomponent Portland cement CEM II and granodiorite aggregate were used. High-calcium fly ash was included in cement and accounts for 14.3% of binder.

Additionally, 14.3% of cement was replaced by siliceous fly ash. Mixture B is made of CEM I 42.5R with granodiorite aggregate. Mixture C is made of CEM II/B-S 32.5R with amphibolite aggregate.

It has been observed that in each case typical temperature evolution is a single-modal function and its properties obviously depend on concrete type and the shape of mould. The admixture of fly ash reduces the maximum temperature in comparison with the reference mixture without ash. Moreover, the time of occurrence of maximum temperature is delayed. The detailed discussion of these issues is presented in authors' previous work<sup>7</sup>.

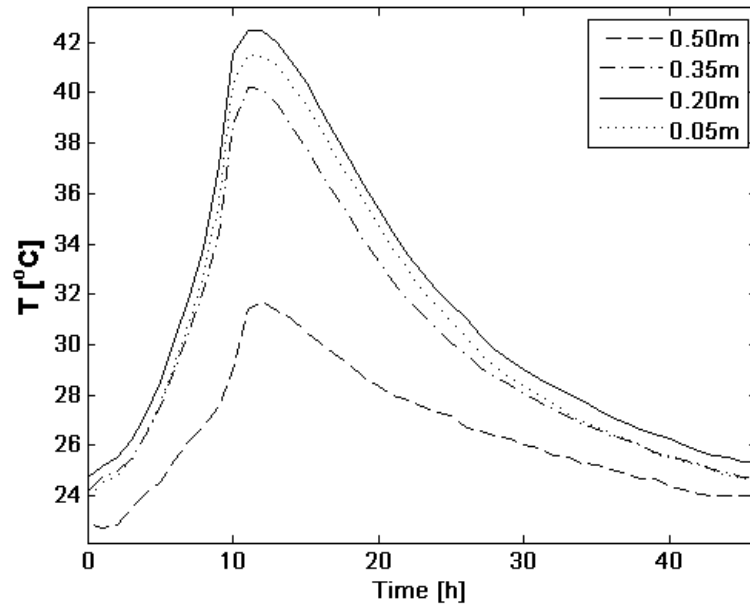


Figure 6: Temperature evolution in time during hardening of concrete in 1D mold – mixture A.

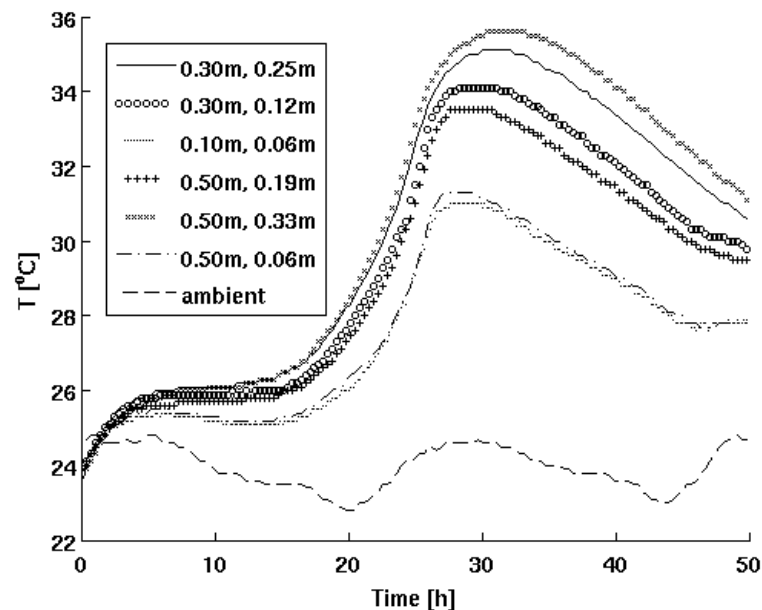


Figure 7: Temperature evolution in time during hardening of concrete in 2D mould – mixture B.

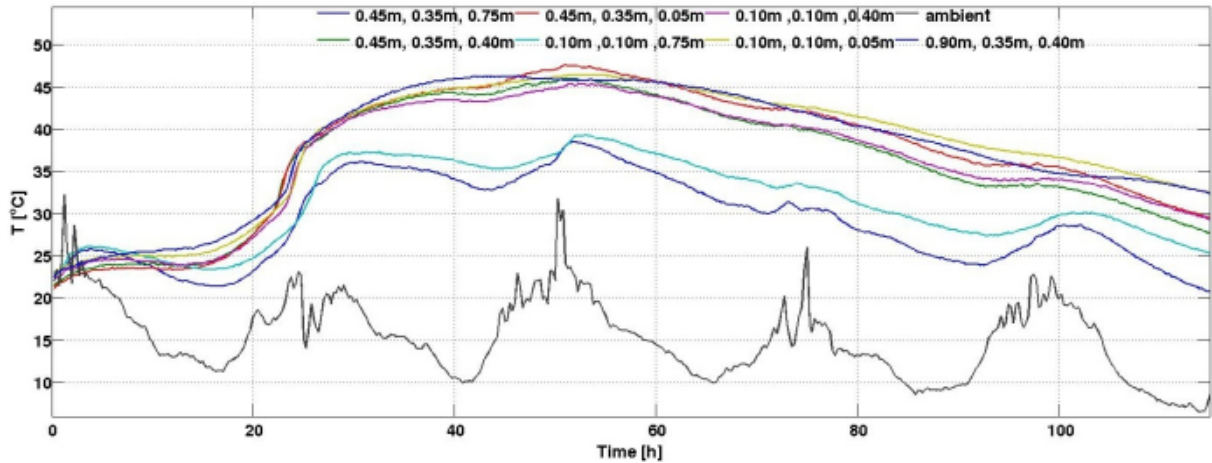


Figure 8: Temperature evolution in time during hardening of concrete in 3D mould – mixture C.

## 7 NUMERICAL RESULTS

The determined heat source production for mixture A is shown in Fig. 9. It was calculated on the basis of 1D temperature measurements (Fig. 6) by means of IHTP. In accordance with previous assumptions the values of heat source were determined in discrete points in time (squares in Fig. 9), but for the purposes of further analysis smooth curve is fitted to these points (solid line in Fig. 9). IHTP solution provides also thermal properties of tested concrete mixture. This information allows to estimate the temperature evolution in two or three dimensional object using in-house FEM software.

Property	Content of components in the mixture [kg/m <sup>3</sup> ]		
	Mixture A	Mixture B	Mixture C
Cement	400	160	280
Sand 0-2mm	580	547	546
Coarse aggregate 2-8mm	625	625	566
Coarse aggregate 8-16mm	615	615	699
High-calcium fly ash	Included in cement	240	120
Water	200	200	200
Superplasticizer	0	6	0

Table 3: Composition of concrete mixtures.

Also based on the determined values the temperature distribution in long cylindrical slab of concrete cooled by piped water is calculated. Temperature distribution in concrete cylinder is shown in Fig. 10. The cylinder is 20m long, with radius of 0.25m and cooling pipe of diameter 0.1m. Temperature distribution 10h after setting is presented, for water flow from left to right. It

can be observed that temperature rise in pipe is significant and in this case it was around 10°C. As intuitively expected, the most effective heat removal from concrete occurs at the beginning of concrete sleeve.

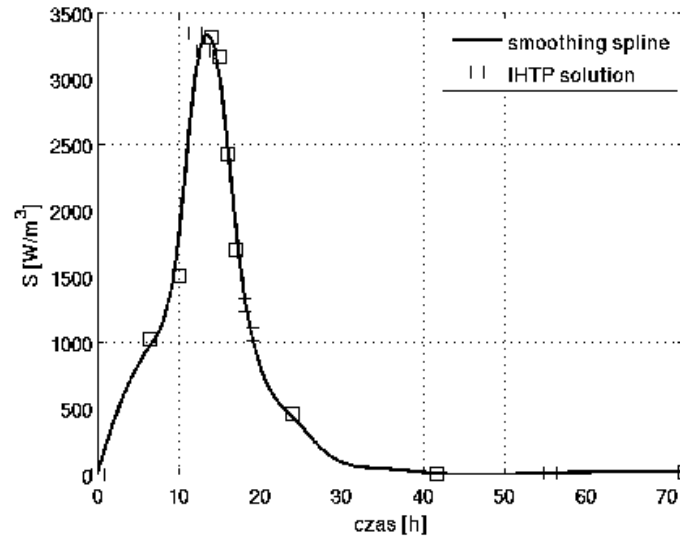


Figure 9: Heat production estimated on the basis of IHTP solution.

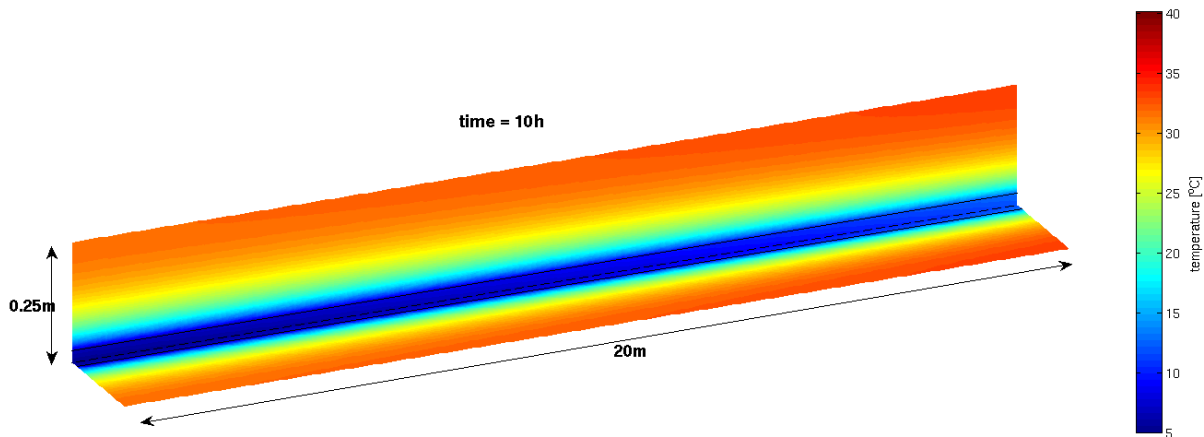


Figure 10: Result of example cooling.

Sample results of the model are shown in Fig. 10. They are qualitatively good, so in the next step they can be treated as an input to the optimization problem. In Fig. 11 the objective function is shown with respect to the inlet water temperature, pipe radius and concrete sleeve radius. Colours represent the value of this function (average temperature difference per unit length). The range of pipe radius was set to 0.01-0.1m, radius of concrete sleeve was set to 0.2-1m with constant length of 20m and initial temperature of water was in the range of 1-50°C. The initial temperature of concrete was 25°C and thermal properties of concrete came from IHTP solution for mixture A. The result confirms the earlier insights that the lowest value of objective function is reached for pipe radius 0.01m, sleeve radius 0.2m and inlet temperature 1°C. Thus, the final result should not be chosen as a minimal value of the objective function, but as an intermediate value, acceptable from the engineering point of view. That obviously leads to the ambiguity of solution, but it should not be read as a drawback of the proposed approach, as it will leave the final decision to the construction engineer. It should also be remembered that the objective

function depends on time. Thus, in solving the optimization problem one cannot be focused only on the desired point in time, but on a wider range of time covering at least the period of temperature rise in the analyzed object.

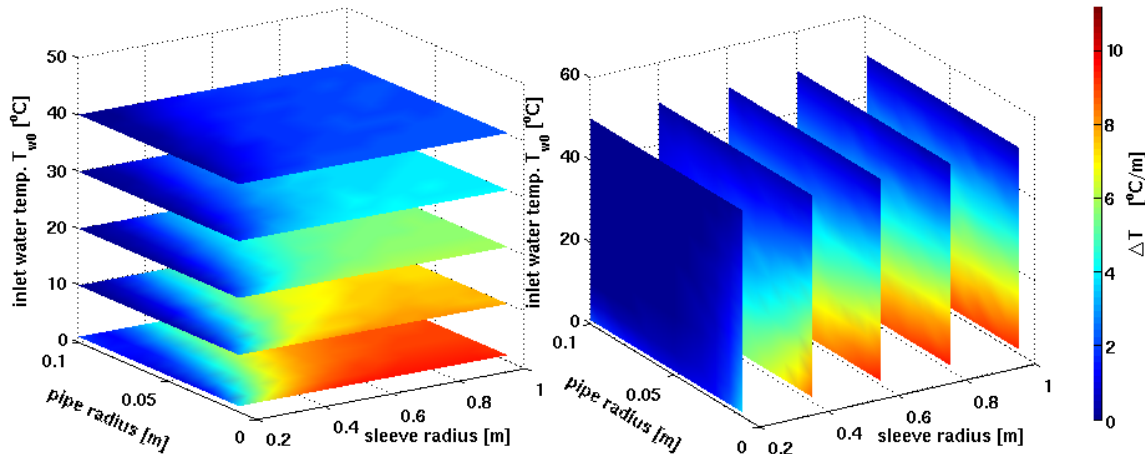


Figure 11: Objective function for optimal cooling system.

## 8 MODEL VALIDATION

In order to validate the numerical model the results of temperature measurements obtained in the experiment have been compared with the calculated values. The compositions of mixtures examined in this section were  $400/552/1278/200 \text{ kg/m}^3$  for mixture D and  $400/580/1240/200 \text{ kg/m}^3$  for mixture E, where consecutive numbers mean cement/sand/coarse aggregate/water amount. CEM I 42.5 was used in both cases, crushed granodiorite was used in mixture D and amphibolite aggregate – in mixture E. The coefficients of heat exchange with the environment have been chosen according to the recommendations found in the literature<sup>18</sup> and are as follows:  $9 \text{ W/m}^2\text{K}$  for the upper, uncovered surface (for trapezoidal blocks and massive block),  $6 \text{ W/m}^2\text{K}$  for the side surface without insulation (in the case of massive blocks),  $1.3 \text{ W/m}^2\text{K}$  for the side surface of the thermal insulation (in the case of massive blocks) and  $0.6 \text{ W/m}^2\text{K}$  surface for the lower mould (in the case of the trapezoid and massive blocks). Calculated temperature field shows fair agreement with the experimentally measured temperature in trapezoid mould (Fig. 12). The result for cross-section through the center of cuboid mould (Fig. 13) also proves that two-dimensional model can be successfully used to calculate temperature in three dimensional objects.

## 9 CONCLUSIONS

Thermal properties of hardening concrete were effectively determined using an unconventional approach – the inverse heat transfer problem solution achieved using 1D temperature measurements and optimization by non-gradient direct search algorithm. Determination of the transient temperature field in hardening concrete is possible for the unknown mix composition. The obtained simulation results are consistent with experimental data, which indicates that this procedure can be adequate in real size structure. Determining thermal properties of concrete materials will enable, in practice, more accurate modelling of temperature fields in massive concrete structure. Calculated temperature field can be helpful at the designing stage of the object, because this information can be included in the project, e.g. by using additional reinforcement. The solution gives also hints how to design an optimal cooling system. Of course the cooling model and optimization of cooling system is very simplified. First of all the model should be better fitted to the real structures and there is also a possibility of introducing many more criteria such as pipe material, thickness of pipe wall, the flow rate of water as well as to include some precooling issues.

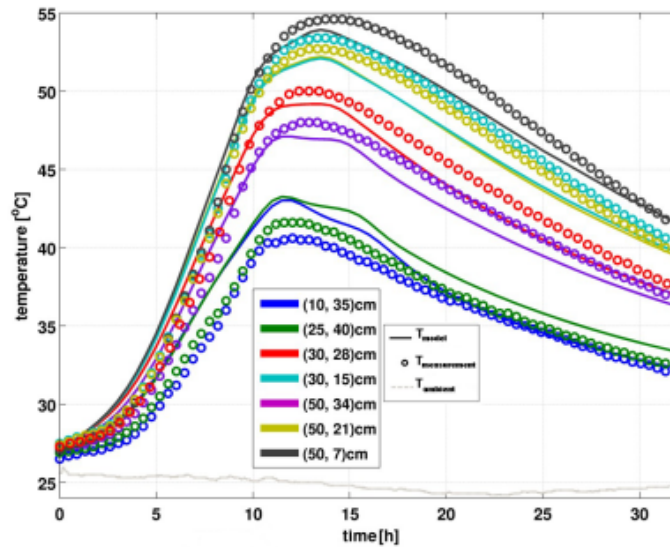


Figure 12: Temperature evolution in 2D mould – mixture D (the numbers in the legend indicate the position of temperature sensors).

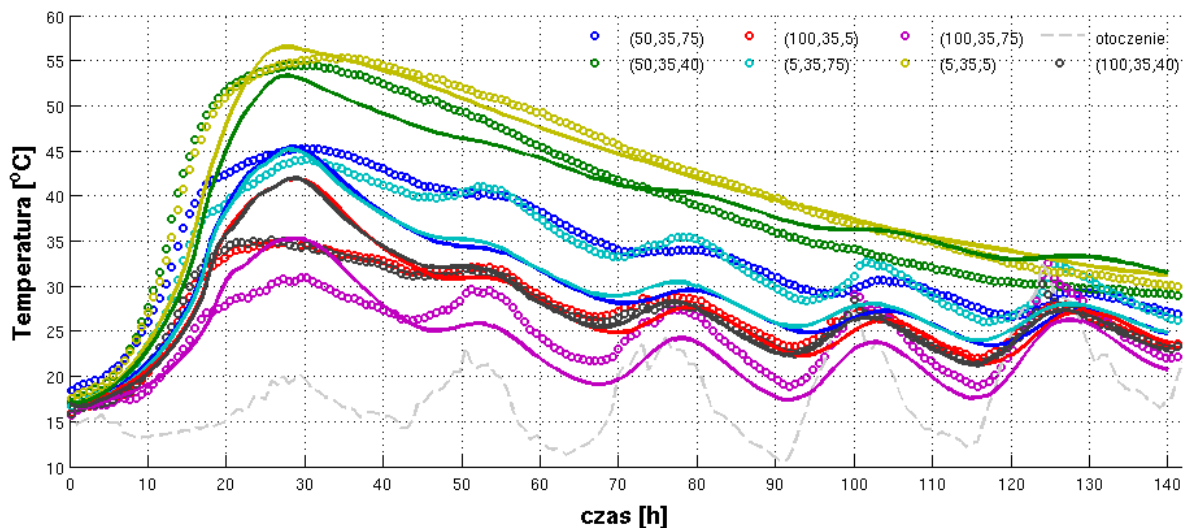


Figure 13: Temperature evolution in 3D mould – mixture E (the numbers in the legend indicate the position of temperature sensors).

## ACKNOWLEDGEMENTS

The authors gratefully acknowledge financial support through the FP7 EU project Smart-Nest (PIAPP-GA-2011-28499) and project financed from the funds of the National Science Centre (Poland) allocated on the basis of the decision number DEC - 2012/05/B/ST8/02971. The collaboration with M. A. Glinicki, Z. Ranachowski and A. Ossowski is also gratefully acknowledged.

## REFERENCES

- [1] Council of Ministers of the Republic of Poland, *National Research Program. Assumptions of science and technology policy and innovation policy*, Resolution, 16 August (2011)
- [2] U.S. Geological Survey, *Mineral Commodity Summaries 2012*, Reston, Virginia (2012)
- [3] Holland T., *Silica Fume User's Manual*, Silica Fume Association, (2005)
- [4] R. Siddique, *Waste Materials and By-Products in Concrete*, Springer, Berlin (2008)
- [5] R. Siddique, M. I. Khan, *Supplementary Cementing Materials*, Springer, Berlin (2011)
- [6] Baran T., Drożdż W., Pichniarczyk P., *The use of calcareous fly ash in cement and concrete manufacture*, *Cement-Lime-Concrete*, 1, 2012, 50-56
- [7] Knor G., Glinicki M.A., Holnicki-Szulc J., Ossowski A., Ranachowski Z., *Influence of calcareous fly ash on the temperature of concrete in massive elements during the first 72 hours of hardening*, *Roads and Bridges*, 12, 1, pp.113-126, (2013)
- [8] Knor G., Glinicki M. A., Holnicki-Szulc J., *Determination of thermal properties of hardening concrete by means of inverse problem solution*, *Roads and Bridges*, 11, 4, pp. 281-294, (2012)
- [9] Audet Ch., Dennis J.E. Jr., *Analysis of Generalized Pattern Searches*, *SIAM Journal on Optimization*, 13, 3, pp. 889–903, (2003)
- [10] ACI Committee, 207.4R-05: *Cooling and Insulating Systems for Mass Concrete*, (2012)
- [11] ACI Committee, 207.1R-05: *Guide to Mass Concrete*, (2005)
- [12] Myers, T.G., Fowkes N.D., Ballim Y., *Modeling the Cooling of Concrete by Piped Water*, *Journal of Engineering Mechanics*, 135, pp. 1375-1383, (2009)
- [13] Charpin, J., Myers, T.G., Fitt, A.D., Fowkes, N.D., Ballim, Y., Patini, A.P., *Piped Water Cooling of Concrete Dams*, *Mathematics in Industry Study Group, Johannesburg*, 1, pp. 69-85, (2004)
- [14] Fowkes N.D., Bassom A.P., *Piped water cooling of concrete: An exercise in scaling*, *Australasian Journal of Engineering Education*, 15(2), 51-58, (2009)
- [15] Brandt A.M., Dąbrowski M., Dębowski T. Glinicki M.A., Holnicki-Szulc J., Knor G., Ossowski A., Ranachowski Z., Sobczak M., *The technique of identification of the transport of heat in the hardening concrete elements*, POIG structural project report "Innovative cement binders and concretes using calcium fly ash", Warsaw, (2011) (in Polish)
- [16] Ballim Y., *A numerical model and associated calorimeter for predicting temperature profiles in mass concrete*, *Cement & Concrete Composites*, 26, pp. 695-703, (2004)
- [17] Hastie, T. J., Tibshirani, R. J., *Generalized Additive Models*, Chapman and Hall. ISBN 0-412-34390-8, (1990)
- [18] Yun L., Myoung-Sung C., Seong-Tae Y., Jin-Keun K., *Experimental study on the convective heat transfer coefficient of early-age concrete*, *Cement and Concrete Composites*, 31, 1, pp. 60-71, (2009)